Bimolecular Networks and Supramolecular Traps on Au(111)

L. M. A. Perdigão,[†] E. W. Perkins,[†] J. Ma,[†] P. A. Staniec,[†] B. L. Rogers,[†] N. R. Champness,[‡] and P. H. Beton*[,†]

Schools of Physics & Astronomy and Chemistry, University of Nottingham, Nottingham, NG7 2RD, U.K.

Received: January 4, 2006; In Final Form: April 27, 2006

We demonstrate the formation of intermixed phases and self assembled molecular templates on the Au(111) surface. The templates are stabilized by hydrogen bonding between melamine molecules with trigonal symmetry and linear PTCDI (perylene tetra-carboxylic di-imide) molecules. When annealed, these molecules spontaneously form either a chiral intermixed phase or a honeycomb arrangement in which vertexes and edges correspond respectively to melamine and PTCDI molecules. We also observe minority phases with more complex intermolecular junctions. The use of these networks as templates is demonstrated by the controlled capture of fullerenes within the pores of the network to form dimers, hexamers, and heptamers. Our results confirm that bimolecular templates can be realized on a range of substrates.

Introduction

Recent advances in two-dimensional self assembly have led to a new type of nanostructured template formed by arrays of nanoscale holes, or pores.[1−4] It has been demonstrated that these pores can be used to trap diffusing molecular species, promoting the growth of novel clusters in cavities with controlled nanoscale dimensions. These arrays have several attractive features. They form spontaneously under suitable preparation conditions and have dimensions which are smaller than those attainable with conventional processing techniques such as electron beam lithography. In addition, their structure is controlled on a molecular scale, raising the possibility of combining chemical functionality with spatial control on the nanometer scale.[5]

In this paper, we show that bimolecular honeycomb arrays stabilized by hydrogen bonding, which we have previously demonstrated can be used to template molecular adsorption on a passivated semiconductor surface, can also be formed on metallic surfaces such as gold with relatively minor changes in the preparation conditions. The templating action on gold is confirmed by the formation of fullerene dimers, hexamers, and heptamers. The network is formed by sequential deposition of perylene tetra-carboxylic di-imide (PTCDI) and melamine on a clean Au(111) surface under ultrahigh vacuum (UHV) conditions followed by annealing (see Figure 1 for molecular structure). As well as the honeycomb arrangement in which melamine acts as a trigonal molecular vertex, we also see a chiral intermixed phase and small regions stabilized by more complex molecular vertexes.

Experimental Methods

A Au(111) surface is prepared by loading a 5 mm × 10 mm piece of gold on mica (purchased from Molecular Imaging Inc.) into an UHV system with a base pressure of 1×10^{-10} torr. The gold film has large (∼100 nm), flat (111) terraces and is cleaned using Ar ion sputtering (1 kV, 1−3 μA) followed by annealing at 150−450 °C for several hours. PTCDI and melamine are sublimed onto the gold surface with the substrate held at room temperature. Images of the surface are acquired using a scanning tunneling microscope (STM) housed within the UHV system and operating at room temperature. Electrochemically etched tungsten tips, cleaned using electron beam heating, were used.

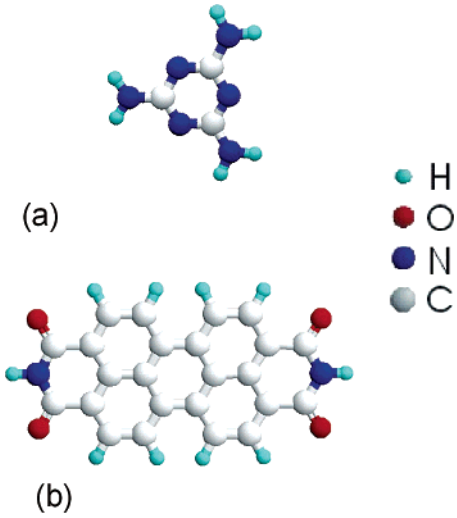

Figure 1. Molecular structure of (a) melamine and (b) PTCDI.

Results

Following the sputter−anneal cycle, we observe the characteristic $22 \times \sqrt{3}$ chevron reconstruction of the Au(111) surface[6] in our STM images. The supramolecular template is formed by depositing 0.1−0.3 monolayers of PTCDI followed by ∼0.5 monolayers of melamine. Figure 2 shows STM images of the surface after deposition of PTCDI and subsequent images acquired after the deposition of melamine. The PTCDI forms ordered islands in which molecules are ordered in a head-to-tail arrangement in rows similar to those previously observed for PTCDI and the closely related NTCDI (naphthalene tetracarboxylic di-imide) on the Ag−Si(111)$\sqrt{3} \times \sqrt{3}$R30° sur-

* Corresponding author. E-mail: Peter.beton@nottingham.ac.uk. Tel.: +44 115 951 5129. Fax: +44 115 951 5180.
[†] School of Physics & Astronomy.
[‡] School of Chemistry.

10.1021/jp060062x CCC: $33.50
Published on Web 06/08/2006

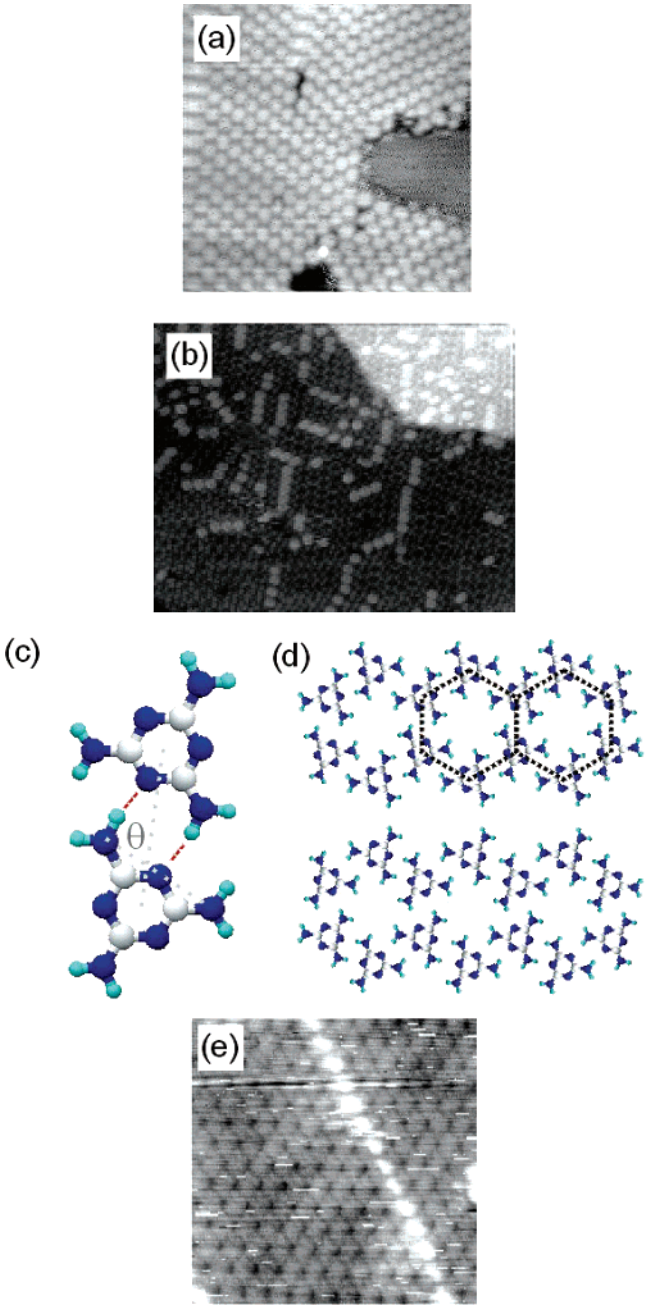

Figure 2. (a) STM image of PTCDI on Au(111); 197 Å × 197 Å, +1.8V, 0.05 nA. (b) Melamine coadsorbed with PTCDI prior to annealing; 320 Å × 240 Å, +1.8 V, 0.2 nA. (c) H bonded arrangement of melamine pairs in which N−H...N hydrogen bonds are identified by red dotted lines. (d) Schematic of the hexagonal ordered array of melamine showing two chiralities. (e) Zoomed area of melamine array; 130 Å × 130 Å, −1.7 V, 0.05 nA.

face[7,8] (Figure 2a). Following deposition of melamine, the PTCDI islands become partially disrupted and we observe a hexagonal arrangement corresponding to ordered arrays of melamine molecules within which isolated PTCDI molecules, or rows of PTCDI molecules, are embedded (see Figure 2b).

We propose that the ordered melamine arrangement is stabilized by a double hydrogen bond similar to that observed in bulk melamine[9] and shown in Figure 2c. An extended honeycomb arrangement is built up by placing the melamine pair on a hexagonal lattice as shown in Figure 2d. The angle between the edges of the molecules and the line connecting their centers, θ, (see Figure 2c) and the separation of the two molecules, d, have been calculated using density functional

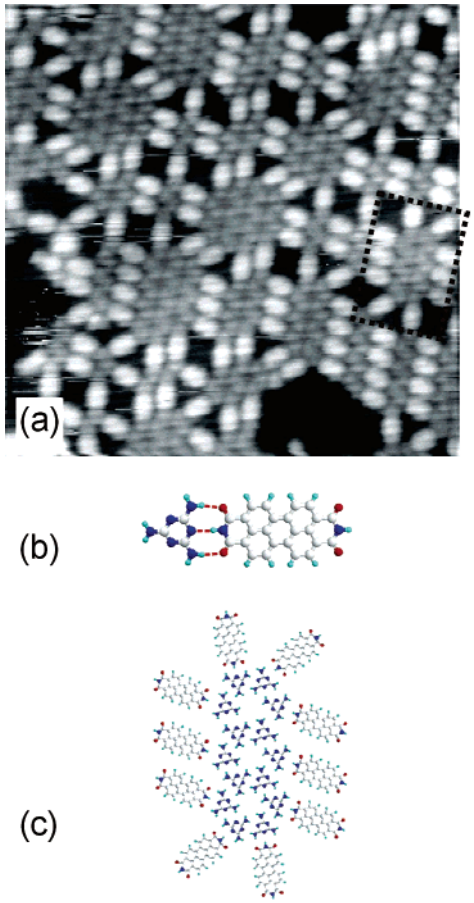

Figure 3. (a) Intermixed PTCDI−melamine phase formed after annealing at ∼ 50 °C, 197 Å × 197 Å, −1.8 V, 0.05 nA showing melamine islands around which PTCDI molecules are attached through hydrogen bonding. (b) Triple hydrogen bond formed between melamine and PTCDI. (c) Schematic of the PTCDI attachment to the melamine array—this corresponds to the region marked by dotted lines in part a.

calculations (using a method which is identical to our previous approach for related molecules[10]) and are found to be $d = 6.08$ Å, and $\theta = 66.5°$, respectively. A higher resolution image of the melamine array is shown in Figure 2e. From the calculated value of d, we predict the period of the melamine array to be $\sqrt{3}d = 10.53$ Å, in good agreement with the measured value, 10.9 ± 0.2 Å.

The proposed melamine structure is chiral. Although it is difficult to resolve this chirality in Figure 2e, it is clearly revealed after the sample has been annealed at ∼50 °C—see the STM image in Figure 3. Following annealing, there is a much greater degree of intermixing between melamine and PTCDI. We observe much smaller melamine islands with PTCDI molecules adsorbed around their edges and forming a bridge to neighboring islands. The PTCDI−melamine interaction is stabilized through the formation of three hydrogen bonds as shown schematically in Figure 3b and c. The chirality results in a tilt of the PTCDI molecules at a constant angle with respect to the edge of the island. Note that all of the interconnected islands in Figure 3a have the same chirality. Intermixed layers with chirality have recently been reported by a number of authors,[11−13] and our structure is most closely related to the arrangements observed by De Feyter et al.[13] at the liquid/solid interface.

Annealing the sample in the range 60−80 °C results in the formation of a hexagonal network (see Figure 4a and b). Nearly all the melamine is desorbed after this annealing step, leaving

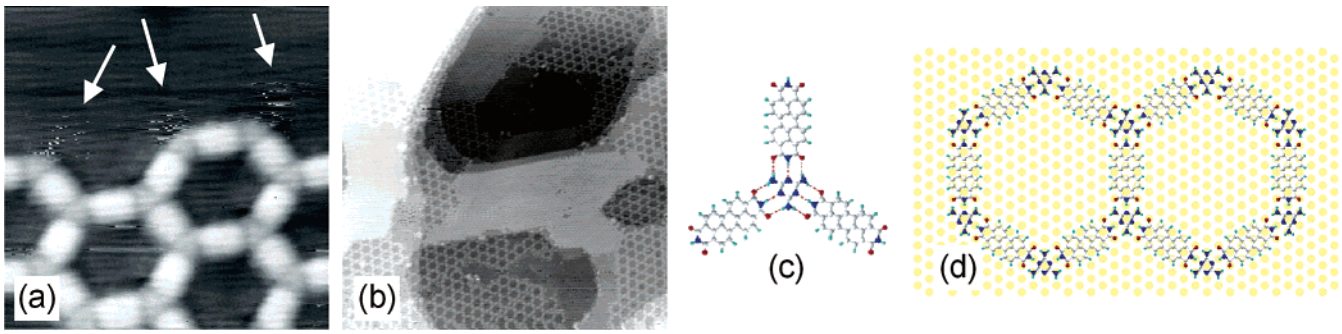

Figure 4. (a) STM image showing the hexagonal PTCDI−melamine network in which PTCDI resolved as brighter rectangular features forming network edges and melamine is the triangular lower contrast network vertex. Arrows identify positions of temporary stabilization of PTCDI; 88 Å × 88 Å, −1.4 V, 0.05 nA. (b) Larger area image of network showing different areas on different gold terraces; 984 Å × 984 Å, −1.4 V, 0.05 nA. (c) Schematic of triangular melamine−PTCDI vertex stabilized by hydrogen binding. (d) Hexagonal network overlaid on gold substrate.

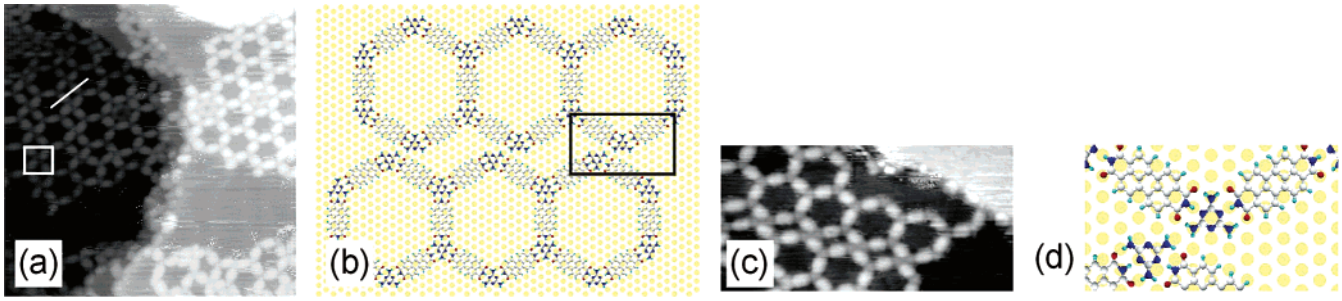

Figure 5. (a) Alternative melamine−PTCDI packing in which vertexes between four PTCDI molecules are formed (e.g., highlighted area). The white bar shows the separation of hexagons referred to in the text; 306 Å × 306 Å, −1.4 V, 0.05 nA. (b) Schematic of the proposed arrangement for a four PTCDI junction overlaid on gold. (c) Higher resolution image of 4-fold junctions; 190 Å × 75 Å, −1.8 V, 0.05 nA. (d) More detailed schematic of area highlighted in part b.

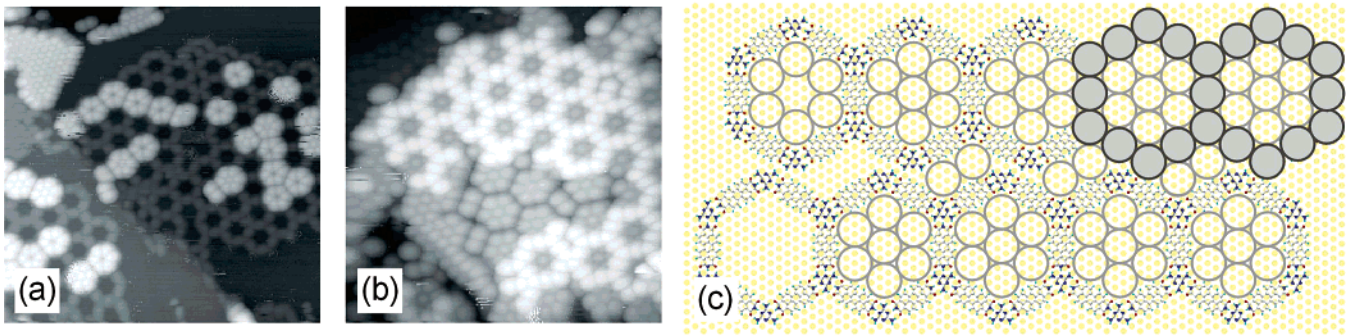

Figure 6. (a) STM image of C_{60} clusters, predominantly hexamers, captured in pores of the supramolecular network; 394 Å × 394 Å, −2.0 V, 0.05 nA. (b) Image of ~1 monolayer of C_{60} on network−pores are filled with either heptamers or dimers depending on the pore size and whether an overlayer of C_{60} forms on the network; 273 Å × 273 Å, −2.0 V, 0.05 nA. (c) Schematic showing C_{60} dimers, hexamers, and heptamers captured within network pores (large open circles) and fullerene overlayer formed on top of network molecules (filled circles).

only molecules trapped at the vertexes or cavities of the network. Figure 4b shows several domains of the network all of which are aligned in the same orientation. Many domains of the network are bound by terrace edges, but growth is not continuous across steps. From our images, we find that the principal axis of the molecular honeycomb is parallel to the $[11\bar{2}]$ direction of the Au(111) surface. The common alignment of the different domains of the network provides strong evidence that network and substrate dimensions are commensurate. From analysis of our images, we deduce that the period of the honeycomb network is $7\sqrt{3}a = 35.0$ Å where $a = 2.885$ Å is the surface lattice constant of gold. We see no evidence for the presence of the $22 \times \sqrt{3}$ reconstruction beneath the molecular network, and in our model for adsorption, we therefore assume that this reconstruction is lifted as has previously been observed following the adsorption of large organic molecules such as fullerenes.[14] Figure 4c shows the hydrogen bonding geometry between a melamine molecule, which forms the vertex of the molecular network, and three PTCDI molecules which form the network edges. Figure 4d shows a schematic diagram with the PTCDI/melamine molecular structure overlaid on the unreconstructed gold surface. The separation between melamine vertex molecules (corresponding to the length of the network edge) is equal to $7a$ (20.2 Å), very close to the value (19.95 Å) observed for the equivalent structure on Ag−Si(111)$\sqrt{3} \times \sqrt{3}$R30°.[1] The structural schematic should be compared with Figure 4a in which the melamine is clearly resolved as a triangular vertex and PTCDI is resolved as the brighter edge. Further interesting features are the noisy features close to the melamine molecules at the edge of the network (see the arrows in Figure 4a). This is attributed to the presence of diffusing PTCDI which is temporarily stabilized at these vertex positions.

We also observe small regions with a different ordering as shown in Figure 5. These often appear at the edges of the

hexagonal network or between regions with different registry and correspond to neighboring hexagons having a common vertex rather than a common edge. From our images, we infer that the separation of hexagon centers (as marked in Figure 5a) is $21\sqrt{3}a/2$ in such regions. A schematic showing the molecular organization in these regions is shown in Figure 5b, and a high resolution image in which this structure is resolved is shown in Figure 5c. We propose that this vertex is stabilized by the more complex H bonding interaction shown in Figure 5d in which the oxygen atoms of PTCDI interact with hydrogen atoms on the amine groups of two melamine molecules.

We have investigated the potential of the pores within the bimolecular network for templating further adsorbed molecular layers. Figure 6 shows clearly that fullerene (C_{60}) molecules are trapped within the network pores. After the deposition of ~0.1 monolayers (Figure 6a), approximately 75% of the pores are completely unoccupied, while the remainder are filled with regular fullerene clusters. This indicates that fullerenes can diffuse across the network but nucleate growth within the pores. The most prevalent cluster is an open hexamer with a small number of heptamers also forming (see Figure 6c for a schematic diagram of molecular placement). The absence of smaller, less symmetric clusters indicates that under our experimental conditions they are kinetically unstable.

At higher coverage (Figure 6b), the hexamers are converted to heptamers and a further fullerene layer grows over the top of the PTCDI−melamine network. Also apparent, and of particular interest in Figure 6b, is the presence of a number of isolated dimers. These smaller clusters, also observed at lower coverage, are captured within the parallelogram shaped pores formed in the defect structures shown in Figure 5. The presence of the dimers indicates that the potential for the capture of adsorbed species in networks of this type does not require the regular hexagonal geometry and matching of pore size to the dimensions of particularly stable clusters such as the fullerene heptamer. The high proportion of hexamers observed indicates that fullerene adsorption at the cavity edge is more favorable than the fullerene−fullerene interaction. This contrasts with our previous observations for the passivated Ag−Si(111)$\sqrt{3} \times \sqrt{3}$R30° surface for which very few open hexamers were observed.

Discussion and Conclusion

The close similarity between the network properties on this surface and our previous results is remarkable and highly significant. As discussed in our introductory remarks, the use of self assembly and noncovalent interactions to control supramolecular assembly on surfaces provides a route to the spatial control of chemical functionality on a molecular scale with many potential areas of application. We have also recently demonstrated that the dimensions of this type of network may be controlled in a rational manner through selection of the component molecules of the network.[15] Taken in combination with the transferability of this process between different substrates, and the demonstration of trapping of species other than C_{60},[4] we argue that our approach to templating has the potential to develop into a method for trapping molecules on a wide range of surfaces with spatial organization on the sub-nanometer scale.

Acknowledgment. We are grateful to the UK Engineering and Physical Sciences Research Council (EPSRC) for financial support under Grant GR/S97521/01. J.M. and E.W.P. were supported through EPSRC Grant GR/R34608/01 and the European Union Framework 6 Grant "Nanomesh", respectively.

References and Notes

(1) Theobald, J. A.; Oxtoby, N. S.; Phillips, M. A.; Champness, N. R.; Beton, P. H. *Nature* **2003**, *424*, 1029−31.
(2) Corso, M.; Auwarter, W.; Muntwiler, M.; Tamai, A.; Greber, T.; Osterwalder, J. *Science* **2004**, *303*, 217−220.
(3) Stepanow, S.; Lingenfelder, M.; Dmitriev, A.; Spillmann, H.; Delvigne, E.; Lin, N.; Deng, X. B.; Cai, C. Z.; Barth, J. V.; Kern, K. *Nature Mater.* **2004**, *3*, 229−33.
(4) Theobald, J. A.; Oxtoby, N. S.; Champness, N. R.; Beton, P. H. *Langmuir* **2005**, *21*, 2038−2041.
(5) De Feyter, S.; De Schryver, F. C. *Chem. Soc. Rev.* **2003**, *32*, 139−150.
(6) Barth, J. V.; Brune, H.; Ertl, G.; Behm, R. J.; *Phys. Rev. B* **1990**, *42*, 9307−18.
(7) Swarbrick, J. C.; Ma, J.; Theobald, J. A.; Oxtoby, N. S.; O'Shea, J. N.; Champness, N. R.; Beton, P. H. *J. Phys. Chem. B* **2005**, *109*, 12167−74.
(8) Keeling, D. L.; Oxtoby, N. S.; Wilson, C.; Humphry, M. J.; Champness, N. R.; Beton, P. H. *Nano Lett.* **2003**, *3*, 9−12.
(9) Cousson, A.; Nicolai, B.; Fillaux, F. *Acta Crystallogr., Sect. E* **2005**, 61, o222−4.
(10) Ma, J.; Rogers, B. L.; Humphry, M. J.; Ring, D. J.; Goretzki, G.; Champness, N. R.; Beton, P. H. *J. Phys. Chem. B* **2006**, *110*, 12207−12210.
(11) de Wild, M.; Berner, S.; Suzuki, H.; Yanagi, H.; Schlettwein, D.; Ivan, S.; Baratoff, A.; Guentherodt, H.-J.; Jung, T. A. *ChemPhysChem* **2002**, *3*, 881−5.
(12) Xu, B.; Tao, C.; Cullen, W. G.; Reutt-Robey, J. E.; Williams, E. D. *Nano Lett.* **2005**, *5*, 2207−11.
(13) Jonkheijm, P.; Miura, A.; Zdanowska, M.; Hoeben, F. J. M.; De Feyter, S.; Schenning, A. P. H. J.; de Schryver, F. C.; Meijer, E. W. *Angew. Chem., Int. Ed.* **2004**, *43*, 74−8.
(14) Altman, E. I.; Colton, R. J. *Phys. Rev. B* **1993**, *48*, 18244−9.
(15) Perdigão, L. M. A.; Champness, N. R.; Beton, P. H. *Chem. Commun.* **2006**, 538−540.